MODELING OF THE IMAGE TRANSFER IN OPTOELECTRONIC SYSTEMS FOR OBSERVATIONS IN TURBID MEDIA

I.E. Astakhov, V.P. Budak, D.V. Lisitsin, and S.Yu. Sukhorosov

Power Institute, Moscow
Received June 11, 1993

In this paper we present expressions derived for mathematical simulation of the process of image transfer in optoelectronic observational systems (OEOS). Such systems include, as their linear components, atmospheric and water channels and allow for the state of the air-water interface, the geometry of its illumination, and the parameters of the source of light and of the optical detector. We consider a scheme of observations, most interesting from the practical point of view, when a narrow beam receiver scans targets illuminated by a broad beam source. It is shown that an effect of enhanced backscattering may be observed in a transparent medium and large scale correlated waves. Computational results are compared to observational data. To estimate OEOS quality, we use detection and identification probabilities for a test target observed against an additive background. We analyze the dependences of these probabilities on the position of a layer of high turbidity between the target and the OEOS, when observations take place in the McClatchey-Fenn atmosphere. It is shown that when such a layer moves from target to observer, the detection probability monotonically decreases, while identification attempts may, depending on the angular size of the target, result in the tracing-paper effect, the t-effect, or a monotonic increase of identification probability.

A wide class of problems of atmospheric optics and hydrooptics deals with estimating of the quality of active and passive optoelectronic observational systems (OEOS), intended for observations through air and water layers with randomly rough interface (RRI). Two aspects of this problem may be separated out.

First, one has to model the structure of an image in an OEOS involving, as its linear elements, the atmosphere and water including the state of the air-water interface, the geometry of its illumination, and parameters of a light source (LS) and of an optical detector (OD).[1]

Second, an integral quality criterion is needed, which would be related to the basic characteristics of the structure of image, and make it possible to compare different OEOSs between each other and to standard, and also to support, improve, and recover image quality during their processing.[2]

Progress in developing graphic packages on PCs drastically modifies the process of simulation and estimation of the OEOS quality bringing it to a new level of automated workstations (AWS) for researchers, suitable for both field and laboratory operations. AWS software must combine a flexible user interface with a capability of quickly and interactively presenting the data in their graphic, tabulated, or image form. We analyze a feasibility of creation of such a system.

Contributions coming to the total distribution of brightness in the plane of analysis of OEOS from multiple scattering and multiple reflections of radiation from target and RRI are of different orders of magnitude. The basis for identification of those components which noticeably affect the structure of the image and for their separation out from the total signal is given by the theory of the operator of optical transfer (OOT) of the OEOS. This operator is constructed based on decomposition of the general boundary-value problem for the equation of radiation transfer (ERT) into the elementary problems.[1] By choosing the small-angle modification of the technique of spherical harmonics (TSH) to find the Green's functions for ERT,[3] one may account for the anisotropy and multiple scattering and obtain convenient analytical expressions enabling the construction of quick computational algorithms.

After averaging over all the possible realizations and taking into account the receiving aperture, the signal takes the form[1]

$$\langle P_R(\hat{n}_S, \hat{n}_R)\rangle =$$

$$= \frac{\Phi_0}{\pi} \int \rho(\mathbf{r}')\, \omega_R(\hat{\mathbf{n}}_R \to \hat{\mathbf{l}}_R)\, l^a(\mathbf{r}_2, \hat{\mathbf{l}}_2' \to \mathbf{r}_R, \hat{\mathbf{l}}_R) O_1(\mathbf{r}'; \mathbf{r}_1, \hat{\mathbf{l}}_1' \to \mathbf{r}_2, \hat{\mathbf{l}}_2') \times$$

$$\times\, l^a(\mathbf{r}_S, \hat{\mathbf{l}}_S' \to \mathbf{r}_1, \hat{\mathbf{l}}_1')\, \omega_S(\hat{\mathbf{n}}_S \to \hat{\mathbf{l}}_S) d\hat{\mathbf{l}}_1' d\hat{\mathbf{l}}_2' d\hat{\mathbf{l}}_S d\hat{\mathbf{l}}_R d^2 r_1\, d^2 r_2 d^2 r', \quad (1)$$

$$O_1(\mathbf{r}'; \mathbf{r}_1, \hat{\mathbf{l}}_1' \to \mathbf{r}_2, \hat{\mathbf{l}}_2') = \frac{t^2}{4(\pi n)^2} \int \Phi(z, \mathbf{k}_1)\, \Phi(z, \mathbf{k}_2)\, \theta(\mathbf{k}_1, \mathbf{k}_2, \Gamma) \times$$

$$\times \exp\left[\frac{i}{z} \mathbf{r}'(\mathbf{k}_1 + \mathbf{k}_2) - \frac{i}{z}(\mathbf{r}_1 \mathbf{k}_1 + \mathbf{r}_2 \mathbf{k}_2) - \frac{i}{n}(\mathbf{k}_1 \mathbf{l}_1' - \mathbf{k}_2 \mathbf{l}_2') \right] d^2 k_1 d^2 k_2, \quad (2)$$

$$\theta(\mathbf{k}_1, \mathbf{k}_2, \Gamma) = \exp\left[-\sigma_M^2 \left(\mathbf{k}_1^2 + \mathbf{k}_2^2 + 2\Gamma \mathbf{k}_1 \mathbf{k}_2 \right) \right], \quad \sigma_M^2 = \frac{\sigma^2}{2} \left(\frac{n-1}{n} \right)^2, \quad (3)$$

where O_1 is the first approximation of the operator of image transfer through a RRI and a sea layer; angular brackets denote the operation of statistical averaging; $\hat{\mathbf{n}}_S$ and $\hat{\mathbf{n}}_R$ are unit vectors of aiming of polar diagrams of the

0235-6880/94/06 452-05 $02.00

LS (power Φ_0) and OD, respectively, $\rho(\cdot)$ is the distribution of the reflection coefficient; $l^a(\cdot)$ and $\Phi(\cdot)$ are the Green's functions of the atmospheric and sea layers, respectively; $\theta(.)$ is the double-point characteristic function of roughness (the Mullamaa function); t is the RRI transmission; n is the refractive index of water; σ^2 and Γ are the variance and the correlation coefficients of the RRI slopes.

There exist three possible schemes of forming the image in OEOS[4] Scheme *3* assumes simultaneous scanning of a target by both the LS and OD polar diagrams which makes it possible to improve the image quality. However, this scheme is technically difficult to be performed in practice. Basic computational expressions for scheme *3* were obtained in Ref. 1.

Of a considerable practical interest are schemes *1* and *2*, which assume scanning by a narrow LS (OD) diagram, while the wide OD (LS) diagram is aimed arbitrarily.

Similar to Ref. 1 we neglect atmospheric scattering and assume the spacing between LS and OD to be short. Then we may write for the two beams polar diagrams

$$\omega_S \circ l^a = \omega_S(\hat{\mathbf{n}}_S - \hat{\mathbf{l}}_1')\,\delta(\mathbf{r}_1 - h\,\hat{\mathbf{l}}_1'),\ \omega_R \circ l^a = \omega_R(\hat{\mathbf{n}}_R + \hat{\mathbf{l}}_2')\,\delta(\mathbf{r}_2 + h\,\hat{\mathbf{l}}_2'), \quad (4)$$

where h is the altitude of the system above RRI; $\delta(\cdot)$ is the Dirac delta-function; index $\circ$ denotes the operation of the angular convolution.

By presenting $\omega_S(\cdot)$, $\omega_R(\cdot)$, $\langle P_R\rangle(\cdot)$, and $\rho(\cdot)$ in terms of their Fourier transforms, and similar to Ref. 1 we obtain for scheme *2* ($\boldsymbol{n}_S = 0$, $\omega_{S.} \gg \omega_R$) with the account of Eqs. (1)–(4)

$$\langle P_R(\hat{\mathbf{n}}_R)\rangle = \frac{1}{2\pi}\int \langle P_R(\mathbf{p})\rangle \exp(-i\,\mathbf{p}\,\mathbf{n}_R)\,d^2p\,, \quad (5)$$

$$\langle P_R(\mathbf{p})\rangle = \frac{\Phi_0\,t^2}{\pi\,n^2\,h^2}\int \tilde{\rho}\left(\frac{2\,\mathbf{K}}{z}\right)\omega_R(\mathbf{p})\,\omega_S\left(\frac{2\,H\,\mathbf{K}}{z} - \mathbf{p}\right)\times$$

$$\times\,\theta(\mathbf{K},\,\mathbf{k},\,\Gamma)\,\Phi(z,\,\mathbf{K} + 0.5\,\mathbf{k})\,\Phi(z,\,\mathbf{K} - 0.5\,\mathbf{k})\times$$

$$\times \exp\left[-i\Delta\mathbf{r}\left[\mathbf{p} - \frac{H}{z}(\mathbf{K} - 0.5\mathbf{k})\right]\Big/ h\right]\exp(-i\mathbf{p}\mathbf{n}_R)\,d^2\Delta r\,d^2K\,d^2k, \quad (6)$$

where $\langle P_R(\mathbf{p})\rangle$, $\tilde{\rho}(2\boldsymbol{K}/z)$ are the spatial spectra of the signal and the target; $\Delta\mathbf{r} = \mathbf{r}_1 - \mathbf{r}_2$, $H = h + z/n$ is the reduced altitude of the OEOS.

Let us transform expression (6) by substituting $\zeta = -\mathbf{p} + \frac{2H\mathbf{K}}{z}$, $\xi = 0.5\frac{H}{z}\,[\mathbf{k} + (\mathbf{p} + \zeta)\,z/H]$, $\beta = \mathrm{D}\mathbf{r}/\mathbf{h}$ to a form more convenient for analysis. Then we obtain

$$\langle P_R(\mathbf{p})\rangle = \frac{\Phi_0\,t^2\,z^4}{\pi\,H^4\,n^2}\,\omega_R(\mathbf{p})\int \tilde{\rho}\left(\frac{\zeta + \mathbf{p}}{H}\right)\omega_S(\zeta)\,\Phi(z,\,\xi\,z/H)\times$$

$$\times\,\Phi[\,z,\,(\mathbf{p} + \zeta - \xi)\,z/H]\exp[\,i\,\beta(\zeta - \xi)]\exp\left[-\sigma_M^2\,[(\zeta + \mathbf{p})^2 +\right.$$

$$\left. + 2(1 - \Gamma)\,\xi(\xi - \zeta - \mathbf{p})]\right]\,d^2\beta\,d^2\zeta\,d^2\xi\,. \quad (7)$$

In the case of scheme *2* (wide LS diagram) we have $\zeta \to 0$. With the account for characteristic scales of the integrands functions variability, which are responsible for contributions from scattering, roughness of the RRI, and from the brightness distribution over the target into the resulting field, we obtain

$$\langle P_R(\mathbf{p})\rangle = \frac{\Phi_0\,t^2\,z^4}{\pi\,H^4\,n^2}\,\tilde{\rho}(\mathbf{p}/H)\,\omega_R(\mathbf{p})\exp\left[-\sigma_M^2\,\mathbf{p}^2\right]\times$$

$$\times\int \omega_S(\zeta)\,\Phi(z,\,\xi\,z/H)\,\Phi[\,z,\,(\mathbf{p} + \zeta - \xi)\,z/H]\times$$

$$\times\exp[i\,\beta(\zeta - \xi)]\exp\left[-2\,\sigma_M^2\,(1 - \Gamma)\,\xi(\xi - \zeta - \mathbf{p})\right]d^2\beta\,d^2\zeta\,d^2\xi\,. \quad (8)$$

In order to lower the order of integration in Eq. (8), we assume, similar to Ref. 1, that

$$\Gamma(\beta) = \begin{cases} 0\,, & \beta > \beta_0\,, \\ 1\,, & \beta \le \beta_0\,. \end{cases}$$

Coming from spectra to original objects, we finally obtain for the statistically averaged OD response to the signal

$$\langle P_R(\hat{\mathbf{n}}_R)\rangle = \frac{1}{2\,\pi^2}\int \tilde{\rho}\,(\mathbf{p}/H)\,F(\mathbf{p})\exp(-i\,\mathbf{p}\,\mathbf{n}_R)\,d^2p\,, \quad (9)$$

$$F(\mathbf{p}) = \Phi_0\,4\,\pi^2\,\frac{t^2\,z^4}{H^4\,n^2}\,\omega_R(\mathbf{p})\times$$

$$\times\,\Phi(z,\,\mathbf{p}\,z/H)\,\Phi(z,\,0)\left\{1 + \frac{\pi\,\beta_0^2}{4\,\pi^2}\int[1 - \exp(-2\sigma_M^2\,\xi(\xi - \mathbf{p})]\times\right.$$

$$\left.\times\,\frac{\Phi[\,z,\,\xi\,z/H]\,\Phi[\,z,\,(\mathbf{p} - \xi)\,z/H]}{\Phi(\,z,\,\mathbf{p}z/H)\,\Phi(z,\,0)}\left[\frac{2\,J_1(\beta_0|\,\xi\,|)}{\beta_0|\,\xi\,|}\right]\mathrm{d}^2\xi\right\}, \quad (10)$$

where $F(\mathbf{p})/F(0)$ corresponds to the optical transmission function (OTF) of the OEOS; J_1 is the first order Bessel function of the first kind. Computational expression for the scheme *1* may be obtained from scheme *2* by substitutions $\omega_R \to \omega_S$ and $\mathbf{n}_R \to \mathbf{n}_S$.

In its structure, expression (10) is similar to that obtained for scheme *1* (see Ref. 1), but it is simpler. The first term is formed by the product of the transmission functions of the medium, roughness, and the spectrum of LS, and it does not account for correlation of radiation at RRI. The second term depends on the effective radius of correlation of RRI slopes $\Delta r_0 = \beta_0/h$ and may, in certain cases, such as a developed swell of a transparent medium, be equal to the first term. The latter corresponds to the effect of valid signal doubling as compared to the case of observation through a flat interface between the two media[5].

The Green's functions from the computational formulas for scheme *2* (*1*) obtained using TSH yield a qualitatively correct description of radiation fields under various meteorological conditions.[6] However, to estimate feasibility and reliability of the developed mathematical model of image transfer in OEOS one apparently needs to compare calculations to data of field experiments.

Figures 1 and 2 compare computations to data from experimental testing of an active OEOS in a laboratory pool of the Institute of Physics of the Academy of Sciences of Byelorussia during the fall of 1989. These experiments were carried out by experts from the Institute of Geochemistry of the Russian Academy of Sciences. During the experiment diffuse images were recorded of a white disk 0.5 m in diameter along the

horizontal paths of different lengths, while water was made turbid by latex. This study showed a good agreement between the theory and experiment within wide ranges of optical depths and illuminating beam divergences for both the pulsed and stationary modes of the OEOS operation. Currently such a system for in–water vision is produced by TURN Ltd.

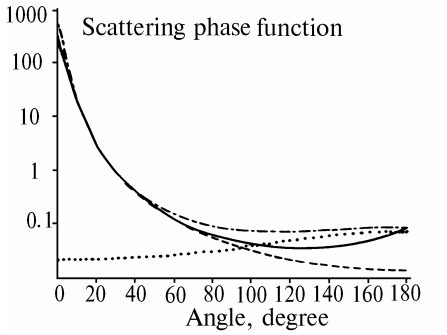

FIG. 1. Approximation of an actual scattering phase function. Latex spheres 1 *μm in diameter. Experiment (solid line), Henji-Greenstein phase function,* $g = 0.94$ (*dashed line*); *Henji-Greenstein phase function,* $g = -0.2$ (*dotted line*); *approximation by two Henji-Greenstein phase functions (dashed-dotted line).*

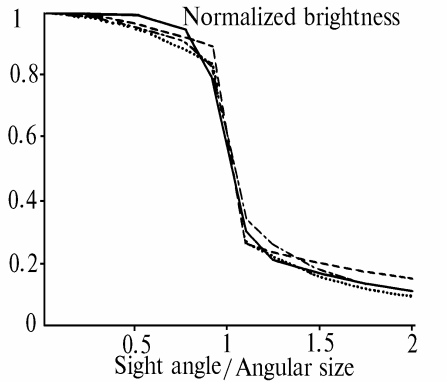

FIG. 2. Normalized distribution of brightness over the input pupil of the OEOS: distance of 30 *m; probability of photon survival of* 0.8. *Extinction of* 0.12 m^{-1}: *experiment (solid line); computations (dotted line); extinction of* 0.2 m^{-1}: *Experiment (dashed-dotted line); computations (dashed line).*

Figure 1 shows the approximation of an actual scattering phase function for latex spheres of 1 μm diameter, used for the modeling purposes. It is approximated by a linear combination of the two Henji-Greenstein phase functions of different asymmetry.

Figure 2 presents the trends of the experimental and computational profiles of normalized brightness of the disk for two optical distances along the horizontal path of observation 30 m long. Modeling showed the shape of the normalized brightness profile to be most sensitive to such characteristics of the medium as single scattering albedo and the scattering phase function. These characteristics should therefore be accurately measured durting field tests of systems of such a kind.

To estimate the quality of OEOS, we analyze the structure of optical image formed by an OEOS, among the basic characteristics of which are the normalized distribution of brightness over the input pupil of the OD (or of illumination over the plane of analysis), the maximum of intensity in the image, the components of optical signal (signals from target and background, from layered "hazes", and speckles from the RRI), OTF or the point spread function (PSF) of the observation system.

In practice, however, it appears inconvenient to use so a large number of parameters to estimate the quality of an OEOS. One would prefer a single integral criterion of OEOS quality, in the form of a number between 0 and 1, which could have a simple analytical expression combining the characteristics of the image and reflecting the main physical effects observed in turbid media easy to be described analytically.

In publications on this problem it is traditional to separate the objective approach to quality estimation and the subjective, one as well as the numerical and functional criteria of such an estimation.[2]

The OEOS OTF is usually selected for its objective functional criterion, while the quantitative measure used is the contrast of an object in the image. However, the applicability of these two measures of system quality is limited, since the task of vision is inherently probabilistic, and the decision whether the target is present within the field of view (i.e., detection) or corresponds to a prescribed type (i.e., identification) is made by the end unit of the OEOS (which may be either an operator or an automatic image analyzer (IA)) on the basis of analysis of *a priori* information, parameters of the input signal, and a certain rule for extracting the signal from noise.

The basis for selection and calculation of the statistical objective criteria of OEOS quality is found in the theory of statistical decisions.[7–9]

We choose the probability of detection P_{det} and identification P_{ident} from a pair of the simplest test-targets set against random, additive, stationary background for the basic numerical objective criteria of the OEOS quality, provided the IA is an optimal linear filter minimizing the functional of the average risk (signal misses and false alarms) in the process of decision making. Such parameters are calculated based on of the theory of statistical decisions. In this case, quality of an actual OEOS is estimated as its closeness to an ideal system implementing the optimal algorithm of signal processing[8].

If it is *a priori* known that the presence or absence of a target in the field of view of the instrument are equally probable, then all the information about the mixture of signal and noise, available from observations, is contained in the likelihood ratio Λ[4,5]. The IA operates according to the decision rule $\Lambda \wedge \Lambda_{\text{th}}$, where Λ_{th} is a certain threshold value of the lihelihood ratio, depending on an artificially selected decision rule and on actual parameters of the OEOS. Rules used in practice differ from each other in the numerical values of Λ_{th}. If the brightness of the object and the background has normall distributions we have in acordance with the theory of optimal linear filtration[9]

$$P = 0.5 \{\text{erfc}\,[(\ln \Lambda - \mu) / 2\sqrt{\mu}] + 1\}\,, \qquad (11)$$

$$\mu = \frac{1}{N} \int [\, L(\mathbf{k}) - L_0(\mathbf{k})]^2\, H^2(\mathbf{k})\, d^2k\,, \qquad (12)$$

where P is the probability of making correct decision during image analysis; μ is the generalized signal-to-noise ratio for a signal detected against the background or identified from a

pair of area-equivalent targets: diffuse disk and diffuse square; $L(\mathbf{k})$ is the spatial spectrum of the signal reaching the IA input from the disk; $L_0(\mathbf{k})$ is mathematical expectation of $L(\mathbf{k})$ for the problem of detection, alternatively, it is the spectrum of the square for the problem of identification; $H(\mathbf{k})$ is the transmission function of the IA; N is the white spectrum of noise, reduced to the input of IA.

Thus, relations (11) and (12) make it possible to calculate the probabilities of detection $P_{\text{det}} = P(\mu_{\text{det}})$ and identification $P_{\text{ident}} = P(\mu_{\text{ident}})$, which are the objective numerical characteristics of the OEOS quality. It is assumed for calculation purposes that $\Lambda_{\text{th}} = 1$, what corresponds to the criterion of an ideal observer;[8,9] the level of noise is assumed to be known also.

As an example of estimation of the quality of an actual OEOS, we analyzed the dependence of P_{det} and P_{ident} on the position of the layer of increased turbidity (100 m thick, optical depth $\tau = 2$) between the target and the passive OEOS at 10 km height in the McClatchey-Fenn model atmosphere.[10] Computations show that while the layer approaches the observer, the values of P_{det} and P_{ident} monotonically decrease (the so-called tracing paper effect). This conclusion is apparent from the analysis of expression (12), since the OTF of the observing system monotonically falls off, while the layer moves toward the IA, the spectrum of the target (the difference spectrum in the case of the identification problem) remains constant.

To include the experimentally observed t–effect[11] into model, we have to redefine the problem of identification of a target from a pair of test-targets for an optimal linear detector as follows. Now IA detects nonlinear perturbations of a target shape while turbid layer moves from target to observer; the sharp image of a target of a known angular size is compared to the current diffuse image, from which the IA has already subtracted the background (i.e. the average brightness at the edge of the OEOS field of view). We believe such an approach to be closer to the physics of the phenomenon, because the IA thus proceeds from the analysis of target types to the analysis of the degree of shape perturbation. To estimate the quality of OEOS with the account for t–efffect, we choose a criterion $P_{\text{OI}} = 1 - P_{\text{det.dif.}}$, where the probability of detecting the difference between the diffuse and the ideally sharp disk, $P_{\text{det.dif.}}$ is directly calculated from Eq. (12). In this case the approach of the turbid layer to the observer produces a nonmonotonic change in P_{OI}, what is caused by t–effect.

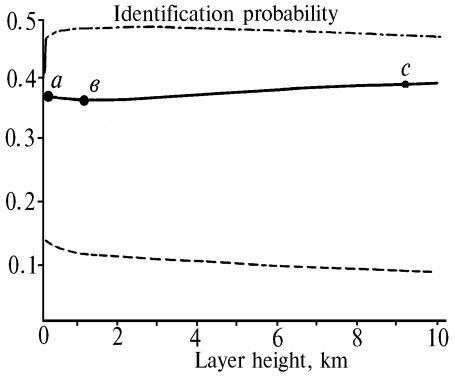

FIG. 3. Identification probability as a function of turbid layer position. Target diameter 50 m *(dashed-dotted line);* 500 m *(solid line); and,* 5 km (*dashed line*); *Characteristic points of the t–effect: height of the layer above the target:* 0.1 (*a*); 1(*b*), *and* 9 km (*c*).

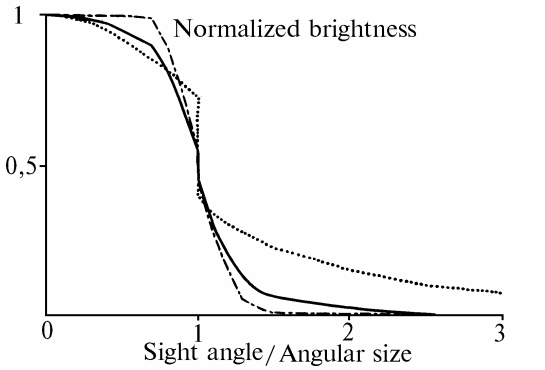

FIG. 4. Normalized distribution of brightness over the input pupil of OEOS during t–effect observation. Target diameter 500 m. *Solid line corresponds to the point a in Fig. 3;dashed-dotted line corresponds to the point b; and, dotted line - to the point c.*

Figures 3 and 4 show computational results for probabilities of identification and for the normalized profiles of brightness for disks of different angular size observed through the atmosphere and through a thin layer of enhanced turbidity. Figure 3 shows that during target identification, while the layer moves from target to observer, either the tracing paper effect or the t–effect or a monotonic growth of the identification probability may take place. Figure 4 presents the normalized profiles of disk brightness for three characteristic points in Fig. 3, which reflect the action of t–effect.

The criterion we used works well only above the threshold, when the level of noise N may be assumed low. Near the threshold the dependence of the form $P_{\text{det.dif.}} \approx 1/N$ results in larger P_{OI} for larger N, and that complicates comparisons between the systems with different noise. Note that the criterion suggested is not fully integral, since it is initially oriented to a bi-alternative problem of vision (see/not see) for a linear IA. Meanwhile an organ of vision (OV) performs nonlinear processing of the image, and it is a multialternative selection among the options, which is more typical for it. Experimental estimates according to the technique of subjective expertise[2] prove this statement.

Physiological optics uses statistical models of the OV,[12–14] which account for its nonlinearity to a certain degree. Therefore it appears feasible to have both experimental and theoretical support for qualitative observations of the t–effect, in the framework of the theory of vision, which will make more strict theoretical basis for statistical estimation of the quality of OEOS from the analysis of image structure.

Note, in conclusion, that formulation of some non-statistical qualitative criterion for any OEOS and any given optical effect, which would imitate nonlinear processing by an OV via common normalization to maximum intensity or a power, logarithmic, or gradient transformation of the image meets no difficulties. However, such a criterion would remain subjective and would lack universality, so that its applicability would be limited by a given system.

Analytical expressions, used to model the structure of images and to estimate the quality of OEOS, provided a basis for developing computer application to support an automated workstation for modelling image transfer in pulsed–active and passive OEOS. Such systems observe their targets through stratified turbid media and account

for correlation of radiation at RRI. A fragment of communication session with such an OEOS is shown in Fig. 5. A multi-window graphic interface provides comprehensive analysis of results in an express regime. Computations were performed using an IBM PC AT.

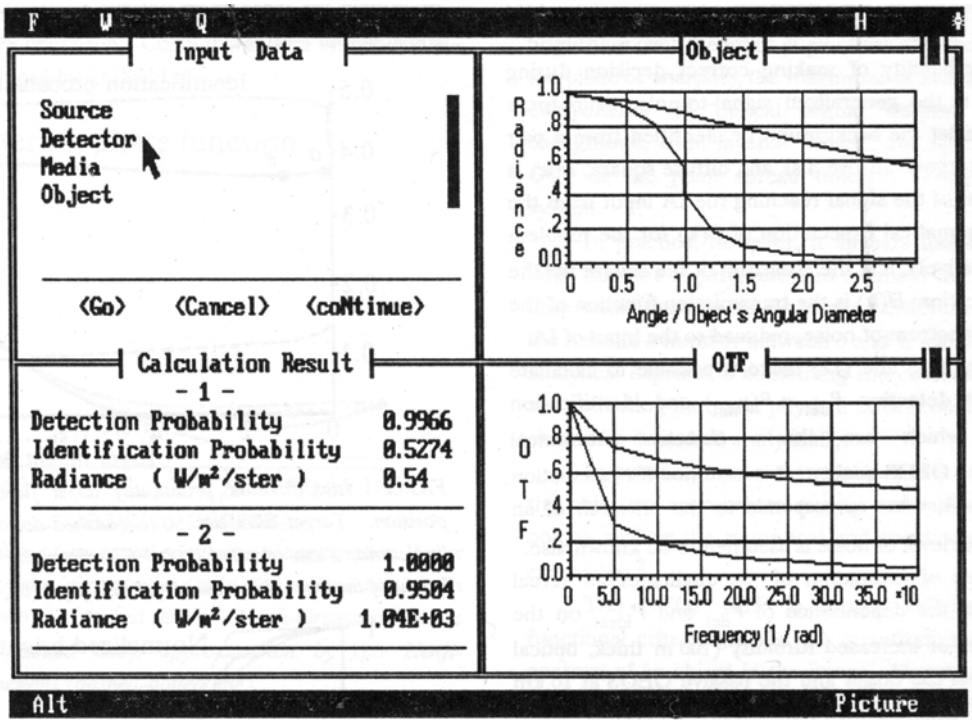

FIG. 5. Fragment of communication session with an AWS modeling image transfer through an OEOS in turbid media

REFERENCES

1. I.E. Astakhov, V.P. Budak, and D.V. Lisitsin, Atmos. Oceanic Opt. **5**, No. 8, 544–549 (1992).
2. U. Pratt, *Digital Image Processing* (Willey, New York, 1978).
3. V.P. Budak and S.E. Sarmin, Atm. Opt. **3**, No. 9, 898–903 (1990).
4. L.S. Dolin and I.M. Levin, *Submarine Vision Handbook* (Gidrometeoizdat, Leningrad, 1991), 229 pp.
5. A.G. Luchinin, Izv. Akad. Nauk SSSR, Fiz. Atmos. Okeana **15**, No. 7, 770 (1979).
6. V.P. Budak, A.A. Ioltukhovsky, I.V. Mishin, and T.Z. Muldashev, in: *Proceeding of Int. Symp. Numer. Transp. Theory*, Moscow (1992), pp. 68–71 .
7. Green and Swets, *Signal Detection Theory and Psychophysics* (Wiley, New York, 1964).
8. N.S Shestov, *Detection of Optical Signals Against the Background of Random Noise* (Sovietskoye Radio, Moscow, 1967), 348 pp.
9. B.R. Levin, *Theoretical Grounds of Statistical Radiotechnology* (Radio i Svyaz', Moscow, 1989), 653 pp.
10. R.A. McClatchey, J. Bolle, and K.Ya Kondratyev, *Report of the IAMAR Radiation Commision Working Group on a Standart Radiation Atmosphere*, Seattle, Washington, USA, August 29, 1977.
11. V.E. Zuev, V.V. Belov, B.D. Borisov, et al.., Dokl. Akad. Nauk SSSR **286**, No. 2, 321–324 (1983).
12. V.N. Martynov and B.I.Shkurskii, Opt Mekh. Promst, No. 7, 6–9 (1982).
13. A.A. Grigoriev and N.F. Koshchavtsev, Tr. Mosk. Energet. Inst., No. 316, 15–18 (1977).
14. A.A. Vas'kovskii and S.S. Romanov, Opt. Mekh. Promst. No. 9 (1987).